King Saud University

Arabian Journal of Chemistry

www.ksu.edu.sa
www.sciencedirect.com

ORIGINAL ARTICLE

DFT calculations, spectroscopic studies, thermal analysis and biological activity of supramolecular Schiff base complexes

Omaima E. Sherif *, **Nora S. Abdel-Kader**

Department of Chemistry, Faculty of Science, Cairo University, Giza, Egypt

Abstract Metal complexes of Schiff base (H_2L) prepared from condensation reaction of o-phenylenediamine and 6-formyl-7-hydroxy-5-methoxy-2-methylbenzopyran-4-one with metal ions: Mn(II), Co(II), Ni(II) and Cu(II) were synthesized. Different analysis tools such as elemental analyses, mass spectra, Fourier transform infrared (FTIR), thermal analysis, conductivity, electronic spectra and magnetic susceptibility measurements are all used to elucidate the structure of the prepared metal complexes. The ligand behaves as a monobasic bidentate in case of mononuclear Ni—HL and Co—HL complexes and acts as dibasic tetradentate in binuclear Mn_2—L and Cu_2—L complexes. All formed complexes are non-electrolytes. The thermal decomposition of Mn_2—L and Co—HL complexes was studied by thermogravimetry/derivative thermogravimetry (TG/DTG). The Schiff base and its complexes were screened for antibacterial activities. The Mn_2—L Complex has the highest antimicrobial activity among the complexes almost close to that of the standard. Density Functional Theory (DFT) calculations at the B3LYP/3-21G level of theory have been carried out to investigate the equilibrium geometry of the ligand. The optimized geometry parameters of the complexes were evaluated using LANL2DZ basis set. Moreover, total energy, energy of HOMO and LUMO and Mullikan atomic charges were calculated. In addition, dipole moment and orientation have been performed.

© 2015 The Authors. Production and hosting by Elsevier B.V. on behalf of King Saud University. This is an open access article under the CC BY-NC-ND license (http://creativecommons.org/licenses/by-nc-nd/4.0/).

1. Introduction

Schiff bases which are derived from the condensation reaction of an amino and carbonyl compounds are considered as an important class of ligands that coordinate to metal ions via azomethine nitrogen. The chemistry of carbon–nitrogen double bond plays a vital role in the progress of chemical science (Gaur, 2003). Schiff bases have a wide applications in many fields such as food industry, dye industry, analytical chemistry,

* Corresponding author at: Department of Chemistry, Faculty of Science, Cairo University, Giza 12613, Egypt. Tel.: +20 10 06045060; fax: +20 2 35728843.
E-mail address: oe_sherif@hotmail.com (O.E. Sherif).
Peer review under responsibility of King Saud University.

Production and hosting by Elsevier

catalysis, fungicidal, agrochemical and biological activities (Brodowska and odyga-Chruścińska, 2014; Wang et al., 1991). The complexes of Schiff bases especially transition metal complexes are the most important stereochemical models in coordination chemistry due to their preparative accessibility and structural variety (Bolos et al., 1998; Keypour et al., 2009; Kuźmin et al., 2005). Metal based Schiff bases have important application in medicinal chemistry (Liu et al., 2008; Yıldırım et al., 2007; Abu-Dief and Mohamed, 2015).

Formyl chromone (benzopyran-4-one) Schiff bases have been the center of attraction for many workers in the current research due to their miscellaneous activities (Di Braccio et al., 2003; Kumar and Koh, 2012; Martens and Mithöfer, 2005). Chromones are naturally occurring compounds which are able to cause cytotoxic effect in various types of cells. They are widely known to have anticancer, antioxidant, antiproliferative, anti HIV, anti-inflammatory and many other activities.

Density Function Theory (DFT) calculations have been carried out to give a systematic theoretical studies and to compare the experimental and calculated results. A limited number of DFT investigations have been carried out on Schiff bases complexes.

Through our continuation to the previously performed work on (chromone) benzopyran-4-one Schiff bases (Sherif and Abdel-Kader, 2014) we report here the preparation and characterization of Mn(II), Co(II), Ni(II) and Cu(II) metal ion complexes of Schiff base derived from condensation of o-phenylenediamine and 6-formyl-7-hydroxy-5-methoxy-2-methylbenzopyran-4-one, Scheme 1. Their structures have been characterized by several tools of analysis. The thermal decomposition of Mn$_2$—L and Co—HL complexes was studied by thermogravimetry/derivative thermogravimetry (TG/DTG). The studies were supported by DFT calculations. The ground state properties and bonding characteristics of the ligand and its complexes were performed using DFT at the B3LYP/3-21G for the ligand and B3LYP/LANL2DZ for its complexes. The Schiff base and its complexes were screened for antibacterial activities using disk-agar diffusion method.

2. Experimental details

All chemicals used in this investigation were chemically pure grade. They included copper (II) acetate (Cu(CH$_3$COO)$_2$·H$_2$O), nickel (II) perchlorate (Ni(ClO$_4$)$_2$·6H$_2$O), cobalt (II) acetate (Co(CH$_3$COO)$_2$·6H$_2$O), manganese (II) chloride (MnCl$_2$·4H$_2$O) (Aldrich), visnagin (Memphis Company for Pharmaceutical and Chemical Industry), potassium dichromate (K$_2$Cr$_2$O$_7$), sodium carbonate (Na$_2$CO$_3$), o-phenylenediamine, sodium hydroxide (NaOH), nitric, hydrochloric and sulfuric acids (El-Nasr Pharmaceutical Chemicals, Adwic). The organic
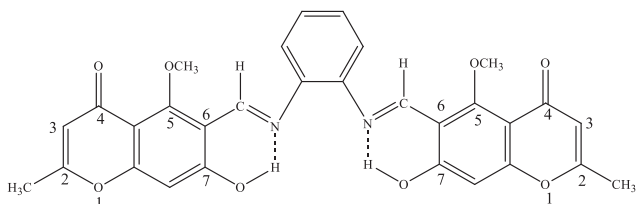
solvents used included ethanol, dimethylformamide (DMF) and dimethylsulfoxide (DMSO). All these solvents were either spectroscopic pure grade solvents from BDH or purified with the recommended methods (Vogel et al., 1989).

2.1. Analysis and physical measurements

Carbon, hydrogen and nitrogen were analyzed by standard microanalysis methods using Automatic analyzer CHNS Vario EL III-Elementar, Germany at Microanalytical center, Cairo University, Giza, Egypt. Mass spectra of the complexes were performed using GC-2010 Shimadzu at Microanalytical center, Cairo University, Giza, Egypt. FTIR spectra were obtained with KBr disk technique using test scan Shimadzu FTIR spectrometer. The spectra were collected in the range 400–4000 cm^{-1}. Molar conductivity of 10^{-3} mol/L solutions of the complexes in DMF was measured on the conductivity meter ORION model 150 of 0.6 cell constant. Thermal analysis of Mn$_2$—L and Co—HL complexes was carried out using TG-50 Shimadzu Thermal Analyzer from ambient temperature to 1000 °C at a heating rate 10 °C min^{-1} in dry nitrogen atmosphere at a flow rate of 30 mL min^{-1} in platinum crucible. The molar Magnetic susceptibility of the chelates was measured at room temperature on prepared samples using a magnetic susceptibility Cambridge England Sherwood Scientific. The effective magnetic moments were calculated from the expression $\mu_{\text{eff}} = 2.828(X_M \cdot T)^{1/2}$ B.M., where X_M is the molar susceptibility corrected using Parcel's constants for diamagnetism of all atoms in the compounds (Emeleus and Sharpe, 1974). The electronic absorption spectra in DMF were measured using automated UV/Vis–NIR 3101 PC Shimadzu spectrophotometer ranged from 200 to 900 nm. The metal content in the prepared chelates was determined by the following wet digestion technique. This is performed by weighing 20–25 mg of the metal chelate, and adding 5 mL of concentrated nitric acid, followed by 5 mL hydrogen peroxide. The solution was heated gently to fumes and then boiled until the solution becomes clear, excess of H$_2$O$_2$ was added if necessary then the solution was diluted with little double distilled water and neutralized with sodium hydroxide solution to pH 5.5 and the metal content was determined by the recommended method (Macdonald and Sirichanya, 1969).

2.2. Synthesis of metal complexes

The solid complexes were prepared by the addition of a hot ethanolic solution containing one mmol of Cu(CH$_3$COO)$_2$·H$_2$O (199 mg), Ni(ClO$_4$)$_2$·6H$_2$O (366 mg), Co(CH$_3$COO)$_2$·6H$_2$O (285 mg) or MnCl$_2$·4H$_2$O (198 mg) to 10 mL ethanolic solution containing one mmol (540 mg) of the Schiff base H$_2$L, m.p. 300 °C (Literature m.p. is 300 °C, (Amin et al., 2012)), Scheme 1, which was synthesized as previously described (Amin et al., 2012). The solution was stirred on a water bath for 2 h during which the metal complex precipitated. The resulting complexes were filtered out and washed thoroughly with successive portions of hot ethanol followed by petroleum ether until the filtrate becomes colorless. The obtained complexes were kept in a vacuum desiccator over anhydrous calcium chloride. The complexes are air stable in the solid state and soluble in DMF or DMSO.

Scheme 1   Schiff base H$_2$L.

Table 1 Analytical and physical data of the ligand, H$_2$L, and its metal complexes.

Symbol	Compound	Formula	MWt (g/mol)	Yield%	Molar conductance (ohm^{-1} cm^2 mol^{-1})	Elemental analyses				
						%C Calcd. (Found)	%H Calcd. (Found)	%N Calcd. (Found)	%Cl Calcd. (Found)	%M Calcd. (Found)
H$_2$L	H$_2$L	C$_{30}$H$_{24}$N$_2$O$_8$	540.52	95	–	66.66 (66.69)	4.48 (4.43)	5.18 (5.20)	–	–
Cu$_2$—L	[Cu$_2$·L·2OH$^-$·2H$_2$O]·2H$_2$O	C$_{30}$H$_{32}$Cu$_2$O$_{14}$N$_2$	771.67	80	26.6	46.69 (46.98)	4.18 (4.16)	3.63 (3.94)	–	16.46 (16.32)
Ni—HL	[Ni·HL·OH$^-$·3H$_2$O]·3H$_2$O	C$_{30}$H$_{36}$NiO$_{15}$N$_2$	722.30	72	19.6	49.88 (49.80)	5.16 (5.06)	3.88 (4.00)	–	8.12 (8.00)
Co—HL	[Co·HL·OH$^-$·3H$_2$O]·H$_2$O	C$_{30}$H$_{32}$CoO$_{13}$N$_2$	686.51	73	15.4	52.49 (52.65)	4.84 (4.82)	4.08 (4.04)	–	8.58 (8.57)
Mn$_2$—L	[Mn$_2$·L·2Cl$^-$·6H$_2$O]·H$_2$O	C$_{30}$H$_{36}$Mn$_2$Cl$_2$O$_{15}$N$_2$	845.39	76	32.3	42.62 (42.41)	4.29 (4.28)	3.31 (3.69)	8.39 (8.35)	12.99 (12.55)

2.3. Biological activity measurement

The antibacterial activities of the Schiff base and its complexes were investigated using the conventional disk-agar diffusion method (El-Gaby, 2004). The activity of the tested samples was studied against the *Staphylococcus aureus* and *Bacillus subtilis* as gram-positive bacteria (G$^+$) and *Pseudomonas aeruginosa* and *Escherichia coli* as gram-negative bacteria (G$^-$) at 20 mg/mL concentration. The bacterial strains were cultured on nutrient agar media. The broth media of bacteria were incubated for 24 h with subsequent filtering of the culture through a thin layer of sterile glass G2. 50 mL of agar media was seeded with 1.00 mL of bacteria and poured into Petri dishes and cooled down to room temperature.

The tested compounds were dissolved in DMSO (which has no inhibition activity) with different concentrations. Sterile uniform size 8 mm diameter filter paper disks (3 disks per compound) were dipped into the dissolved tested compounds and carefully placed on surface of the seeded agar plate. After incubation for 24 h at 37 °C, the diameter of inhibition zone surrounding each disk was measured and used to calculate the mean of inhibition zones. Ampicillin was used as antibacterial standard agent.

2.4. Molecular orbital calculations

In this section, we try to explore the optimized geometrical parameters (bond lengths, bond angles and dihedral angles), net charges on active centers and energetic of the ground state for the ligand (H$_2$L) and its complexes with Mn(II), Co(II), Ni(II) and Cu(II).

In all calculations, Density Functional Theory (DFT) used at the B3LYP level (Becke, 1993), 3-21G (McGrath and Radom, 1991) as a basis set for the ligand and LANL2DZ (Hay and Wadt, 1985) as basis set for the complexes. All calculations were performed using G09 W program (Frisch et al., 2009).

3. Results and discussion

The microanalytical data (C, H, N and metal contents) and some physical properties of the ligand (H$_2$L) and its complexes are listed in Table 1. These complexes are stable in air, non-hygroscopic and have high melting point (> 300 °C), and they are easily soluble in DMF, DMSO and slightly soluble in nonpolar solvents. The analytical data are in good agreement with the proposed stoichiometry of the complexes. The obtained data for the complexes confirm the results (1:1) (M:L) stoichiometry for Ni—HL and Co—HL and (2:1) (M:L) for Cu$_2$—L and Mn$_2$—L complexes. The molar conductance values of the complexes at room temperature in DMF are much lower than the values reported for the (1:1) electrolytes in the same solvents (Geary, 1971), indicating their non-electrolytic nature.

3.1. Mass spectra of metal complexes

The mass spectra were measured in order to confirm the composition and to support the identity of the structure of the prepared metal complexes, Fig. 1. The mass spectra of mononuclear complexes revealed the molecular ion peak at *m/z* 772 (calcd. 722.30) and 686 (calcd. 686.51) for
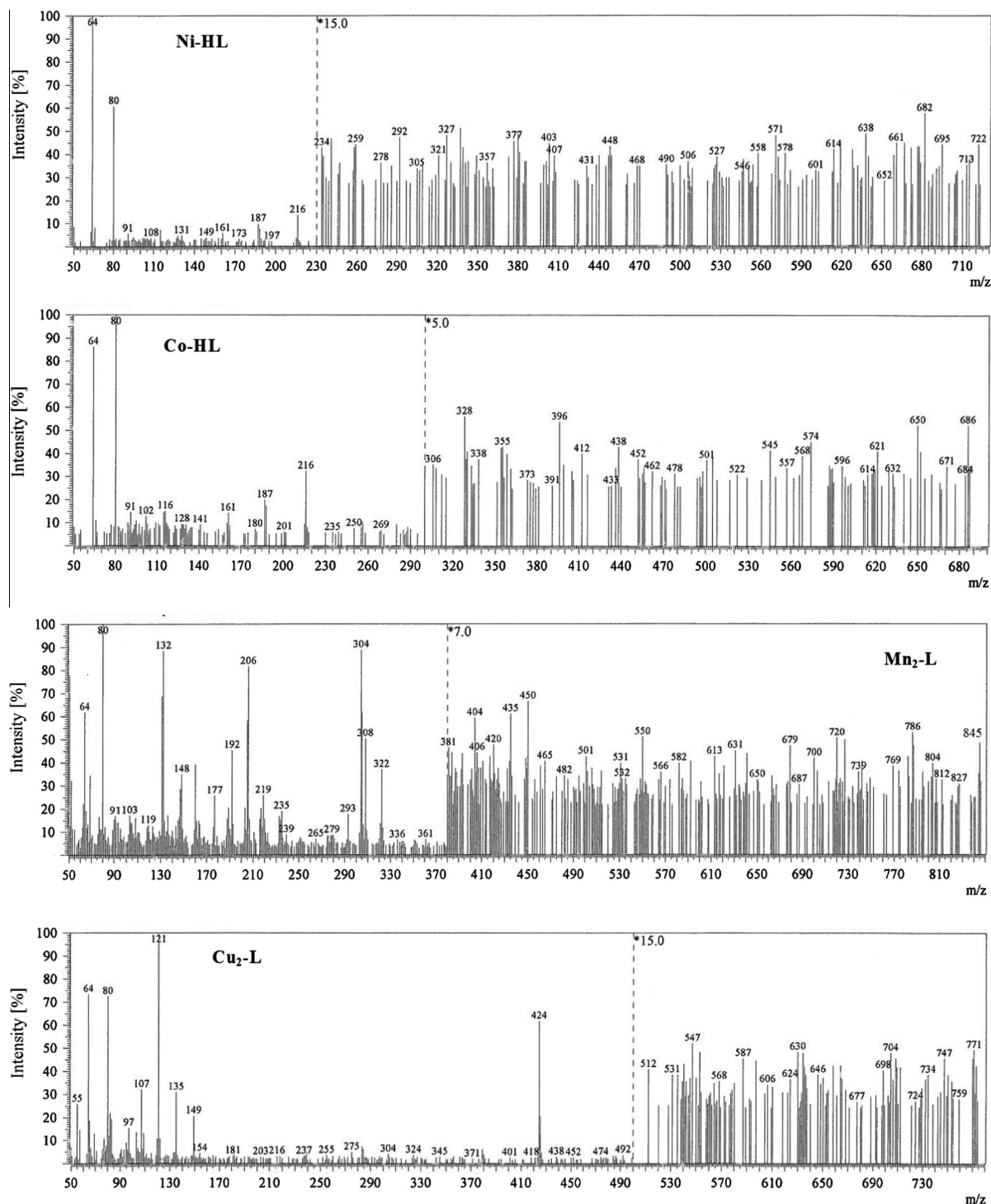
Figure 1 Mass spectra of the metal complexes.

[Ni·HL·OH⁻·3H₂O]·3H₂O and [Co·HL·OH⁻·3H₂O]·H₂O, respectively. In case of binuclear complexes their molecular ion peeks are in agreement with their calculated formulae [Mn₂·L·2Cl⁻·6H₂O]·H₂O and [Cu₂·L·2OH⁻·2H₂O]·2H₂O at m/z 845 (calcd. 845.39) and 771 (calcd. 771.67), respectively.

3.2. FTIR spectra

Table 2 shows the infrared band assignments of Schiff base (H₂L) and its metal chelates.

IR spectra of the complexes were compared with that of the free Schiff base in order to show the bonding sites in the ligand

Table 2 Assignment of IR-bands of Schiff base (H$_2$L) and its metal chelates.

Compound	$\bar{v}$, cm^{-1}					
	$v(C{=}O)_{benzopyrone}$	$v(C{=}N)_{azomethine}$	$v(C{-}O)_{phenolic}$	vOH	vM${-}$O	vM${-}$N
H$_2$L	1675, 1658	1636	1167	3432	–	–
[Ni·HL·OH$^-$·3H$_2$O]·3H$_2$O	1668, 1640	1589	1245	3422	517	430
[Co·HL·OH$^-$·3H$_2$O]·H$_2$O	1667, 1640	1593	1242	3420	517	423
[Cu$_2$·L·2OH$^-$·2H$_2$O]·2H$_2$O	1657, 1640	1589	1241	3420	511	455
[Mn$_2$·L·2Cl$^-$·6H$_2$O] H$_2$O	1656, 1640	1582	1257	3421	542	488
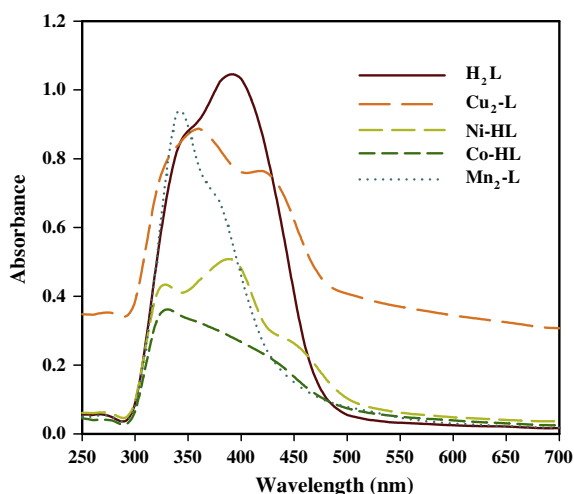
Figure 2 Electronic absorption spectra of Schiff base and its complexes.

Table 3 Electronic absorption bands and magnetic moments of the Schiff base and its metal chelates.

Compounds	v cm^{-1}	B.M.
H$_2$L	29,412, 25,641	–
[Cu$_2$·L·2OH$^-$·2H$_2$O]·2H$_2$O	27,778, 23,474	2.76
[Ni·HL·OH$^-$·3H$_2$O]·3H$_2$O	30,675, 22,026, 25,773	3.33
[Co·HL·OH$^-$·3H$_2$O]·H$_2$O	30,581, 23,041	4.37
[Mn$_2$·L·2Cl$^-$·6H$_2$O] H$_2$O	28,985, 26,316	10.14

that may be involved in the chelation. The discussion was focused on the most important bands v (C{=}O)$_{benzopyrone}$, v (C{=}N)$_{azomethine}$, v (OH) and v (C${-}$O)$_{phenolic}$ in the IR spectrum of the free Schiff base.

The metal complexes contained all the bands from the ligand and also other bands indicative of the coordination of the ligand with the metal ions.

The carbonyl stretching vibration v (C{=}O)$_{benzopyrone}$ of two benzopyran-4-one moieties appeared as two bands in the range 1675–1658 cm^{-1} in the IR spectrum of the ligand (Amin et al., 2012). These bands shifted to lower wave number after complexation due to the perturbing effect of the coordinated metal ions. The shift in binuclear complexes is different from that of mononuclear complexes. In binuclear complexes, the band appears as doublet at lower wave number, Table 2, while in mononuclear complexes, the v (C{=}O)$_{benzopyrone}$ appears as two bands. This means that the coordination of

metal ion to ${-}$C{=}N${-}$ in one side affects the carbonyl of this side, while v (C{=}O)$_{benzopyrone}$ of the unchelated side is slightly changed. However, the band due to v (C{=}N)$_{azomethine}$ at 1636 cm^{-1} in the spectrum of the free ligand shifted to lower frequency (43–54 cm^{-1}) and interfered with the band of stretching frequency of C{=}C in all the metal complexes. This indicates the participation of this group in the complexation (Bradley et al., 1981). This is supported by the appearance of new band in the spectra of all complexes at 423–488 cm^{-1} which is attributed to vM${-}$N stretching (Bradley et al., 1981). The shift, Table 2, occurs in the band at 1167 cm^{-1} (Amin et al., 2012) due to v (C${-}$O)$_{phenolic}$ refers to the coordination through the oxygen of the hydroxyl group in position seven of the benzopyran-4-one moiety and the formation of C${-}$O${-}$M bond (Bellamy, 1975; Saraswat et al., 1977). In the low frequency region, new band observed in the FTIR spectra of all chelates in the region 511–542 cm^{-1} may be attributed to vM${-}$O (Rao, 1963). This in turn, confirms the bond formation between the metal ion and the oxygen of phenolic group of the benzopyran-4-one ring.

The broad band at 3420–3422 cm^{-1} in the IR spectra of all complexes could be attributed to the stretching vibrations of water molecules (Junnosuke et al., 1956; Kemp, 1978). The band at 876–886 cm^{-1} in the FTIR spectra of the complexes is due to the OH bending of the coordinated water molecules. This confirms the presence of the coordinated water molecules (Nakamoto, 1986).

3.3. Electronic absorption spectra and Magnetic susceptibility measurements

The electronic absorption spectra of the metal complexes in dimethylformamide (DMF) are shown in Fig. 2. The electronic absorption spectrum of Schiff base H$_2$L as discussed before (Amin et al., 2012) exhibits a band at 390 nm (25,641 cm^{-1}) which is due to an intramolecular charge transfer (CT transition) involving the whole molecule. Another shoulder appears at 340 nm (29,412 cm^{-1}) in the spectrum of free Schiff base which can be assigned due to the π–π^* transition within the azomethine (CH{=}N) chromophore group (Downing and Urbach, 1969). A bathochromic shift of charge transfer band is observed in the electronic spectra of Cu$_2$${-}$L and Mn$_2$${-}$L complexes at 27,778 and 28,985 cm^{-1}, respectively, while hypsochromic shift is observed in the spectra of Ni${-}$HL and Co${-}$HL complexes at 30,675 and 30,581 cm^{-1}, respectively. This shift confirms the participation of nitrogen atom of azomethine group in the complexation (Sönmez and Sekerci, 2002). The electronic spectra of all complexes show bands in the range of 23,041–26,316 cm^{-1}, Table 3, which may be

mainly due to LMCT transition. The electronic spectrum of Ni—HL complex shows an additional band at 25,773 cm^{-1} attributed to $^3A_{2g} \to {}^3T_{1g}(P)$ transition (Patil et al., 2013) which indicates an octahedral geometry around Ni(II) ion.
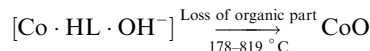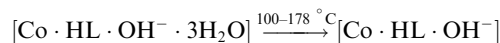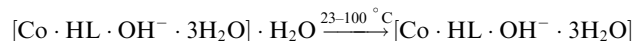
The magnetic moment value of the binuclear complex (2:1) (M:L) Cu$_2$—L complex is 2.76 B.M (1.38 B.M. per metal ion) and this μ_{eff} is consistent with the proposed square planar geometry for the Cu(II) complex (Chohan and Jaffery, 2000). On the other hand, the magnetic moment of Ni—HL complex was (3.33) B.M. This value is within the range (2.9–3.3 BM), found for paramagnetic complex of Ni(II) with octahedral geometry (Nicholls, 1973; Jha and Mukharjee, 2007). The room temperature magnetic moment of the solid cobalt (II) complex lie at 4.37 B.M., indicating the presence of three unpaired electrons (Earnshaw, 1968) in high spin octahedral environment (Chavan et al., 2011; Gudasi et al., 2006) which is in good agreement with the octahedral range 4.3–5.2 BM (Hankare et al., 2004a,b). In addition, the binuclear Mn$_2$—L complex shows high spin paramagnetic moment of 10.14 B. M. (5.07 B.M. per metal ion) corresponding to the presence of five unpaired electrons in an octahedral environment (Thakor et al., 2010).

3.4. Thermogravimetric analysis

Thermogravimetric analyses data, Table 4, were measured from ambient temperature to 1000 °C at a heating rate of 10 °C/min. The TG/DTG curves of Co—HL and Mn$_2$—L complexes are shown in Fig. 3. The first decomposition step was observed in the TG curve of Co—HL complex within the temperature range of 23–100 °C appeared as peak at 50 °C in DTG curve corresponds to the loss of one hydration water molecule with mass loss of 2.73% (calcd. 2.62%). The second step of decomposition in the region 100–178 °C corresponds to

the loss of three coordinated water molecules with mass loss of 7.68% (calcd. 7.87%). This step appeared as peak at 157 °C in the DTG curve of this complex. The loss of organic moiety occurs at the temperature range of 178–819 centered at 475 °C. The complex completes its gradual decomposition till the stable cobalt oxide is formed as a final product above 819 °C.

The thermal decomposition for this complex can be formulated as follows:

$$[Co \cdot HL \cdot OH^- \cdot 3H_2O] \cdot H_2O \xrightarrow{23-100 \ ^\circ C} [Co \cdot HL \cdot OH^- \cdot 3H_2O]$$

$$[Co \cdot HL \cdot OH^- \cdot 3H_2O] \xrightarrow{100-178 \ ^\circ C} [Co \cdot HL \cdot OH^-]$$

$$[Co \cdot HL \cdot OH^-] \xrightarrow[178-819 \ ^\circ C]{Loss \ of \ organic \ part} CoO$$

On the other hand, the loss of one lattice water molecule, mass loss of 2.08% (calcd. 2.13%), occurs at the temperature range of 20–72 °C and appeared as peak at 51 °C in the TG/DTG curve of Mn$_2$—L complex. The mass loss of 12.92% (calcd. 12.78%) in the range 72–159 °C, DTG peak at 100 °C, is due to the elimination of six coordinated water molecules from this complex. The chloride ion was eliminated in the 159–243 °C range (Gaber and Al-Shihry, 2004) with mass loss 8.33, calcd. (8.39%). The organic part decomposes in the range 243–820 °C with DTG peak at 514 °C to give the manganese carbonate, MnCO$_3$ as a final product.

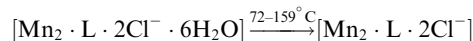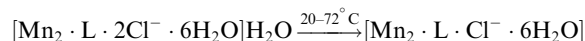On this basis, the thermal decomposition for Mn$_2$—L complex can be formulated as follows:

$$[Mn_2 \cdot L \cdot 2Cl^- \cdot 6H_2O]H_2O \xrightarrow{20-72 \ ^\circ C} [Mn_2 \cdot L \cdot Cl^- \cdot 6H_2O]$$

$$[Mn_2 \cdot L \cdot 2Cl^- \cdot 6H_2O] \xrightarrow{72-159 \ ^\circ C} [Mn_2 \cdot L \cdot 2Cl^-]$$

Table 4 Thermogravimetric analysis data of Mn$_2$—L and Co—HL complexes.

Chelates	Dehydration stage			Decoordination stage			Metal residue%		
	Temp. range	%Weight loss		Temp. range	%Weight loss		Temp. (°C)	Calcd.	Found
		Calcd.	Found		Calcd.	Found			
[Co·HL·OH$^-$·3H$_2$O]·H$_2$O	23–100	2.62	2.73	100–178	7.87	7.68	819	10.91	10.90
[Mn$_2$·L·2Cl$^-$·6H$_2$O]·H$_2$O	20–72	2.13	2.08	72–159	12.78	12.92	820	27.19[a]	26.25[a]

[a] Metal carbonate residue.
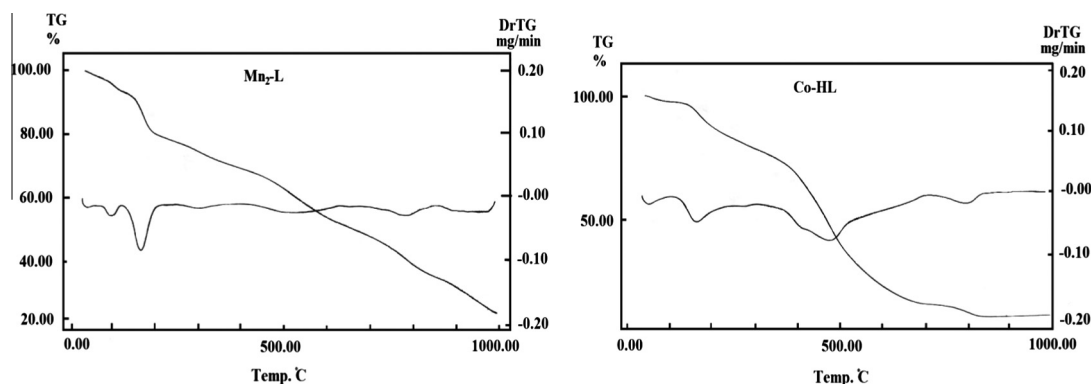
Figure 3 TG/DTG curves of Mn$_2$—L and Co—HL complexes.

$$[Mn_2 \cdot L \cdot 2Cl^-] \xrightarrow{159-243\,^\circ C} [Mn_2 \cdot L]$$

$$[Mn_2 \cdot L] \xrightarrow[243-820\,^\circ C]{\text{Loss of organic part}} [MnCO_3]$$
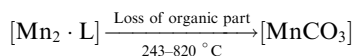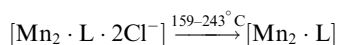
According to elemental analyses data, interpretation of IR spectra, thermal analyses, conductivity, electronic spectra and magnetic susceptibility measurements, it may be concluded that the metal ions coordinated to the Schiff base (HL⁻) via the azomethine nitrogen atom and the oxygen of the deprotonated hydroxyl group in case of (1:1) (M:L) Ni─HL and Co─HL complexes, so the ligand behaves as a monobasic bidentate, Scheme 2. On the other hand, Cu(II) and Mn(II) ions were bonded to L²⁻ ligand through the two C═N groups and the two oxygen of the deprotonated hydroxyl groups to form binuclear (2:1) (M:L) complexes in which the ligand acts as dibasic tetradentate, Scheme 3.

3.5. Geometrical parameters of the ligand

The optimized structure of the ligand is shown in Fig. 4 with numbering of the atoms. The energies of the ground state and the dipole moment computed by B3LYP/3-21G for H_2L are presented in Table 5.

The computed energy gap E_g ($E_{LUMO} - E_{HOMO}$) is an important stability indicator that helps to characterize the chemical reactivity and kinetic stability of the molecule (Rakha et al., 2014). As the E_g decreases the reactivity increases and the amount of electronic charge transfer from the ligand to the central metal ion increases i.e. it easily offers electrons to an acceptor. Low value of energy gap is also due to the groups that enter into conjugation (Rakha et al., 2014). Accordingly, the ligand L²⁻ is more reactive than HL⁻, as reflected from the energy gap values, by 0.215 eV (5.8 kcal). Thus, L²⁻ ligand can act as a
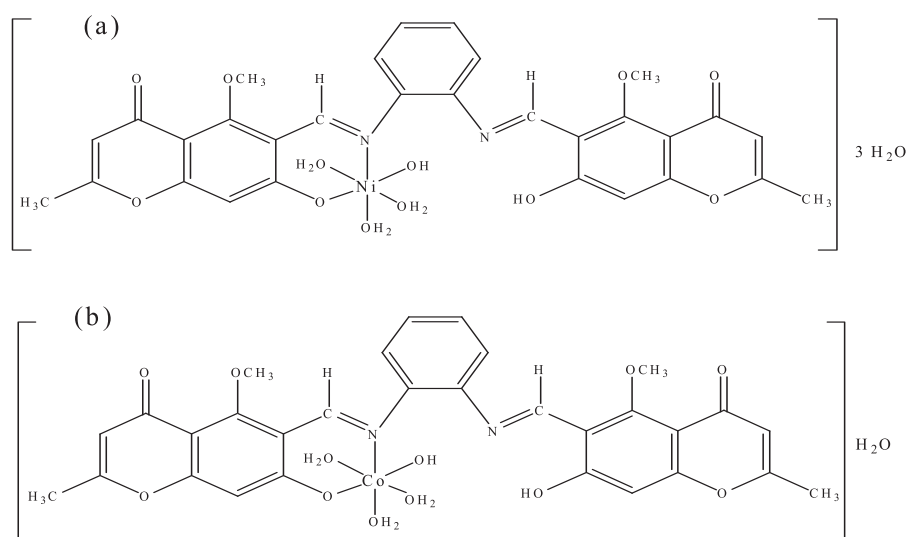
Scheme 2 The proposed structures of (a) Ni─HL and (b) Co─HL complexes.
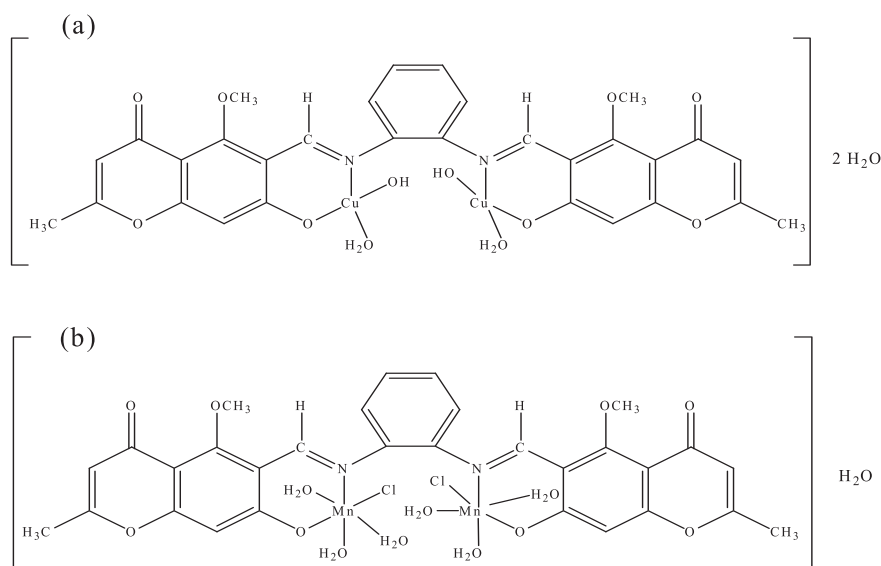
Scheme 3 The proposed structures of (a) Cu₂─L and (b) Mn₂─L complexes.

H_2L

HL^-

L^{2-}
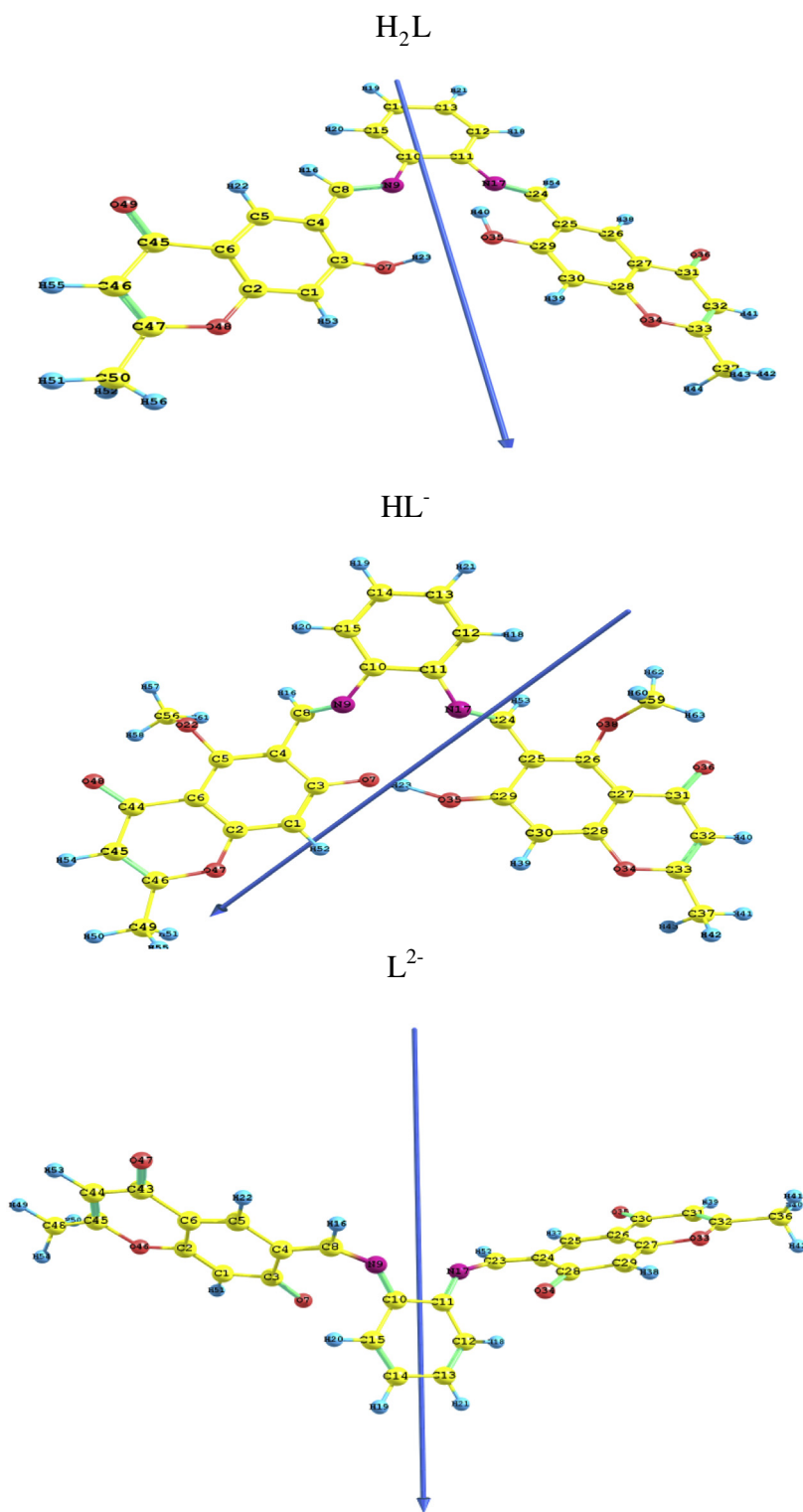
Figure 4   The optimized geometry, vector of dipole moment and numbering system for H_2L using B3LYP/3-21G.

tetradentate ligand and interacts with two metal ions to form binuclear metal complexes in case of Cu_2—L and Mn_2—L. From the computed net charge on the active centers, Table 6, noting that the most negative centers are O7, O35, N9 and N17 hence, the ligand bonded through these active centers.

3.6. Geometrical parameters of the complexes

Tables 5–8 give the values of the energies, dipole moment, energy gap, energy of HOMO and LUMO, net charge on active centers, bond lengths and bond angles of all the complexes under study.

Table 5 Ground state properties of the ligand and its metal complexes using B3LYP/3-21G for ligand and B3LYP/LANL2DZ for complexes.

Parameter	HL$^-$	L^{2-}	Ni—HL	Co—HL	Cu$_2$—L	Mn$_2$—L
E_T, au	−1858.061	−1857.408	−2342.060	−2317.599	−2564.309	−2563.290
E_{HOMO}, au	−0.0777	0.0282	−0.1603	−0.1710	−0.1025	−0.1108
E_{LUMO}, au	0.0490	0.1470	−0.0870	−0.0825	−0.0631	−0.0698
E_g, eV[a]	3.446	3.231	1.994	2.407	1.071	1.115
μ, D	4.061	6.236	9.576	9.052	3.829	10.080

[a] $E_g = E_{LUMO} - E_{HOMO}$.

Table 6 The net charge on active centers of ligand and its complexes.

Center	HL^{-1}	L^{2-}	Ni—HL	Co—HL	Cu$_2$—L	Mn$_2$—L
O7	−0.694	−0.575	−0.380	−0.379	−0.679	−0.771
N9	−0.529	−0.514	−0.354	−0.309	−0.569	−0.486
N17	−0.554	−0.544	−0.455	−0.420	−0.564	−0.570
O35	−0.646	−0.551	−0.456	−0.366	−0.683	−0.705
M1			0.342	0.294	0.826	0.205
M2					0.803	0.291
M1(H$_2$O)						
M—O13			−0.684	−0.707		
M—O14			−0.684	−0.679		
M—O16			−0.509	−0.474		
M—O68					−0.978	
M—O67						−0.889
M—O81						−0.916
M—O65						−0.903
M1(OH)$^-$						
M—O15			−0.630	−0.638		
M—O72					−0.991	
M2(H$_2$O)						
M—O65					−1.015	
M—O74						−0.945
M—O72						−0.908
M—O63						−0.928
M2(OH)						
M—O68					−1.025	
L → M1			1.658	1.706	1.174	1.795
L → M2					1.197	1.709

In addition, Figs. 5 and 6 represent the optimized geometry, numbering system and the vector of the dipole moment for metal complexes using B3LYP/LANL2DZ. In complexes of Co—HL and Ni—HL, the metal coordinates with N9 and O7 while in Cu$_2$—L and Mn$_2$—L with N9, O7, N17 and O35.

The geometric changes that are observed in the ligand moiety itself are interesting. Thus, most of bonds show elongation upon complexation with the metal ions. From the analysis of the data calculated for the bond lengths, Table 7, one can conclude that C8—N9, C3—O7, C24—N17 and C29—O35 bond lengths become longer in all complexes, as the coordination takes place via N atoms of the (C=N)$_{azomethine}$ and the oxygen of the deprotonated hydroxyl groups (El-Gammal, 2010). This finding is due to the formation of the M—O and M—N bonds which make the C—O and C—N bonds weaker (El-Gammal, 2010). The bonds between M and the ligand sites in the complexes i.e. M—N and M—O are long, 1.874 Å for Ni—N9, 1.800 Å for Ni—O7, 1.924 Å for Co—N9, 1.846 Å for Co—O7, 1.862 Å for Cu—N9, 1.921 Å for Cu—O7, 1.902 Å

for Mn-N9 2.151 Å for Mn—O7, 1.850 Å for Cu—N17, 1.931 Å for Cu—O35, 2.018 Å for Mn—N17 and 2.215 Å for Mn—O35 compared to the typical M—X bond lengths which have the values Cu—O 1.62 Å, Cu—N 1.66 Å and Ni—N 1.44 Å (Armelao et al., 2010). The long M—O and M—N bonds in the complexes mean that the ionic character of these bonds is small. Also, the charge on the metal ion in the complex is much less than 2 in Co(II), Ni(II), Cu(II) and Mn(II). Hence, the comparison between the calculated B3LYP/LANL2DZ and the typical M(II)—N and M(II)—O is not very precise. The bond angles of the Schiff base moiety are altered relatively upon coordination but the angles around the metal vary upon changing the metal center. This change affects the other angles, Table 8, which are reduced or increased on complex formation as a consequence of bonding. The bond angles confirm that the Ni—HL, Co—HL and Mn$_2$—L complexes are distorted octahedral with two water molecules occupying the axial positions and the other water molecule and the OH$^-$ or Cl$^-$, required to complete the

Table 7 The optimized bond length, Å, for ligand using B3LYP/3-21G and for complexes using B3LYP/LANL2DZ.

Bond length (Å)	HL$^-$	L^{2-}	Ni—HL	Co—HL	Cu$_2$—L	Mn$_2$—L
C10—C11	1.403	1.408	1.431	1.400	1.421	1.575
C10—N9	1.402	1.410	1.449	1.413	1.424	1.533
C8—N9	1.255	1.266	1.404	1.330	1.320	1.422
C4—C8	1.476	1.465	1.408	1.420	1.424	1.471
C3—C4	1.413	1.462	1.425	1.426	1.449	1.518
C3—O7	1.321	1.238	1.318	1.331	1.320	1.406
C11—N17	1.406	1.411	1.500	1.393	1.421	1.517
C24—N17	1.264	1.270	1.609	1.479	1.324	1.490
C24—C25	1.464	1.458	1.494	1.446	1.421	1.499
C25—C29	1.442	1.467	1.402	1.406	1.448	1.489
C29—O35	1.268	1.233	1.406	1.403	1.321	1.414
M—N9			1.874	1.924	1.862	1.902
M—O7			1.800	1.846	1.921	2.151
M—N17					1.850	2.018
M—O35					1.931	2.215
M(H$_2$O)						
M—O13			2.889	2.254	3.385	2.013
O14			2.065	2.099		2.095
O16			1.975	1.926		2.112
M(OH)						
M—O15			1.740	1.798	1.852	
M2(H$_2$O)					2.319	
MO51						2.044
MO63						2.388
MO72						2.186
M2(OH)					1.839	

Table 8 The optimized bond angles, degrees, for ligand using B3LYP/3-21G and for complexes using B3LYP/LANL2DZ.

Bond angle (°)	HL$^-$	L^{2-}	Ni—HL	Co—HL	Cu$_2$—L	Mn$_2$—L
<C10 N9 C8	125.9	120.0	118.9	120.0	119.8	122.5
<N9 C8 C4	118.9	125.9	128.8	125.9	126.1	129.2
<C8 C4 C3	118.4	120.7	119.8	122.3	121.8	129.6
<C4 C3 O7	120.5	124.6	121.5	122.3	122.8	123.3
<C10 C11 N17	118.1	121.3	144.9	136.3	120.5	124.0
<N17 C24 C25	124.8	119.0	123.3	123.9	126.8	138.9
<C24 C25 C29	122.3	121.8	132.8	124.1	122.9	129.3
<C25 C29 O36	125.5	125.0	115.3	118.1	122.6	119.7
<N9 MO7			96.7	95.8	94.8	107.9
<N17 MO35					96.4	107.8

coordination number of the metal, at the equatorial positions to give octahedral geometry, while Cu$_2$—L complex shows square planar geometry.

The values of the dihedral angles around metal ion in the complexes are far from 0.0° or 180° which indicate that the metal ion is not in the same plane of the donating sites. All the studied complexes are polar as it is evident from the magnitude of their dipole moments, Table 5. As the energy gap of the studied complexes decreases, the reactivity of the complexes increases. The reactivity of the complexes under study follows the order Cu$_2$—L > Mn$_2$—L > Ni—HL > Co—HL.

Table 6 presents the net charge on active centers of the ligand and the studied metal complexes and the amount of charge transferred from the ligand to the central metal ions i.e. L → M. The results of Table 6 show that in Ni—HL and Co—HL complexes, Ni12 and Co12 ends up with a net charge of 0.342 e and 0.294 e, respectively, indicating that the two metal ions received 1.658 e and 1.706 e from their surrounding donating sites of the ligand (O7 and N9). In case of Cu$_2$—L and Mn$_2$—L the charge density increases on the donating atoms after complexation indicating that there is an electron back–donation from the metal ion to the donating sites. These findings are further confirmed by comparing the values of the calculated charge on the donating sites in both the complexes and the free ligand.

So theoretical calculations confirm the results obtained from the above mentioned tools of analysis that the metal ions coordinated to the Schiff base (HL$^-$) via the azomethine nitrogen atom (N9) and the oxygen of the deprotonated hydroxyl group (O7) in case of (1:1) (M:L) Ni—HL and Co—HL complexes and the ligand behaves as a monobasic bidentate, Fig. 5. For binuclear (2:1) (M:L) complexes one metal is coordinated with N9 and O7 and the other metal ion with N17 and O35 indicating that the ligand acts as dibasic tetradentate, Fig. 6.

3.7. Biological activity

The main aim of the production and synthesis of any antimicrobial compound is to inhibit the causal microbe without any side effects on the patients. In addition, it is worthy to stress on the basic idea of applying any chemotherapeutic agent which depends essentially on the specific control of only one biological function and not multiple ones.

In testing the antibacterial activity of the compounds under investigation we used more than one tested organism to increase the chance of detecting antibiotic principles in tested compounds. The antibacterial activity of the Schiff base (H$_2$L) and its metal complexes against *S. aureus* and *B. subtilis* (G$^+$) bacteria and *P. aeruginosa* and *E. coli* as (G$^-$) bacteria were tested, Fig. 7, to inhibit the causal microbe without any side effects on the patients.

The biological activity of the ligand and its metal complexes were also compared with Ampicillin (Antibacterial agent) as a standard. In the present study the ligand, Ni—HL and Cu$_2$—L showed no biological activity towards these types of bacteria, and in other words, they gave no inhibition zone diameters values. The two complexes Co—HL and Mn$_2$—L showed a biological activity towards *S. aureus* and *B. Subtilis* (G$^+$) and *P. aeruginosa and E. coli* (G$^-$) bacteria with inhibition zone diameters ranging from 11–15 and 20–22 mm/mg sample, respectively, Fig. 7. The Mn$_2$—L Complex has the highest antimicrobial activity among the complexes, almost close to that of the standard, Table 9.
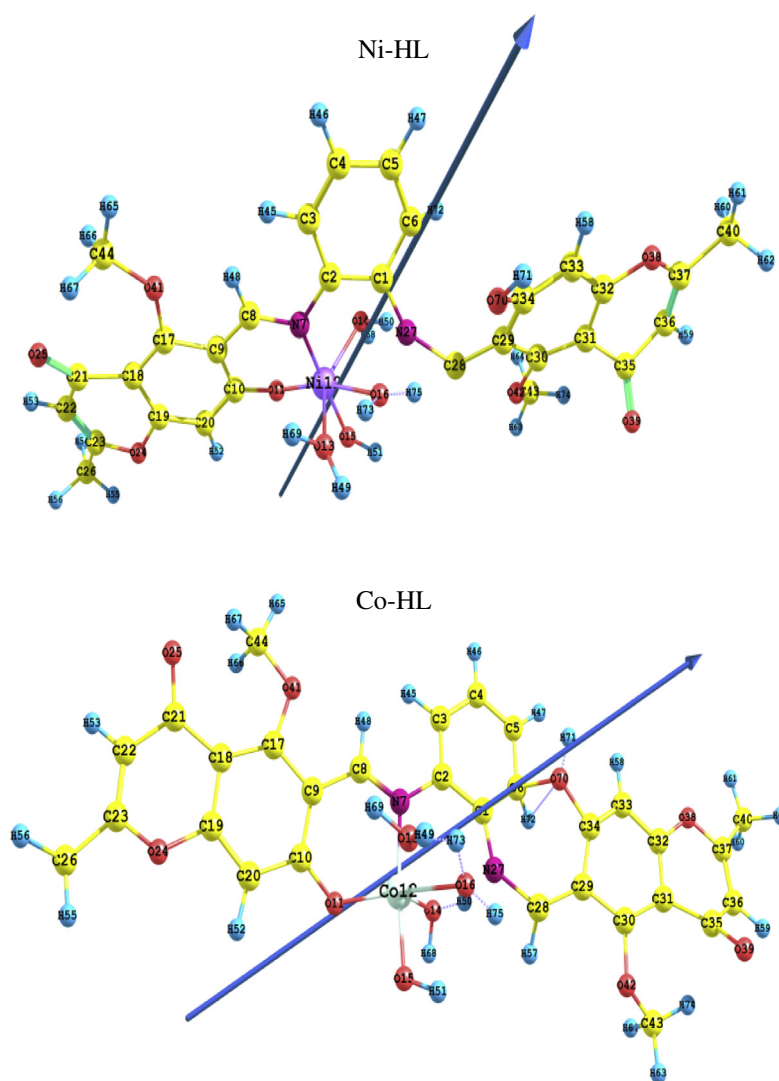
Figure 5 The optimized geometry, numbering system and vector of the dipole moment for Ni—HL and Co—HL complexes using B3LYP/LANL2DZ.

The lipid membrane that surrounds the cell favors the passage of only the lipid-soluble materials, so lipophilicity is an important factor controlling antibacterial activity. This finding suggests that chelation can facilitate the ability of such complexes to cross the cell membrane and can be explained by Tweedy's Chelation Theory (Dharmaraj et al., 2001). On chelation, the polarity of the metal ion will be reduced because of partial sharing of its positive charge with donor groups and the delocalization of π-electrons over the whole chelate ring will be increased. This enhances the lipophilicity of the complex which favors its penetration through the lipid membrane and blocks the metal binding sites in the enzymes of microorganisms.

In other words, the chelates may disturb the respiration process of the microbial cells. This will lead to the inability of the microbial cells to synthesize their own proteins that restrict further growth of the organism. Accordingly, this demonstrates the enhancement of antibacterial activity as a function of chelation. The variation in the activity values of different compounds against different organisms depends on either the impermeability of the cells of the microbes or on the differences in ribosomal structures of microbial cells (Dros et al., 1998). On the other hand, the Ni—HL and Cu$_2$—L complexes have no biological activities. This may be due to lower permeability of these complexes through the microbial cell membrane indicating the decrease of their penetration through the lipid membrane. Hence, they could neither block the enzyme's active site nor inhibit the growth of the microorganisms.

The biological activity of the prepared complexes can be correlated with ground state properties. In spite of, the higher reactivity of Cu$_2$—L complex which can be explained in terms of the energy gap, it has no biological activity. It is found that Mn$_2$—L complex has higher antimicrobial activity than that of the free ligand and the other complexes. Mn$_2$—L complex has the highest dipole moment among the complexes as shown in Table 5. This finding may be one of the reasons for the highest biological activity of this complex.
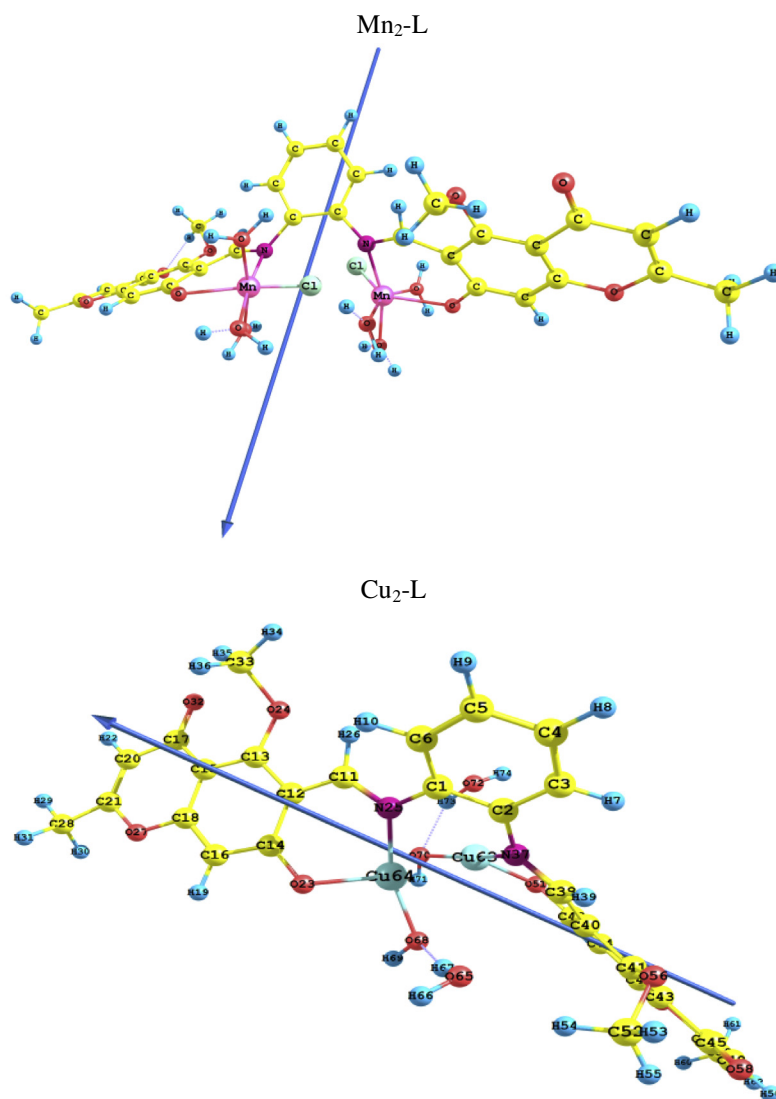
Mn$_2$-L

Cu$_2$-L

Figure 6 The optimized geometry, numbering system and vector of the dipole moment for Mn$_2$—L and Cu$_2$—L complexes using B3LYP/ LANL2DZ.
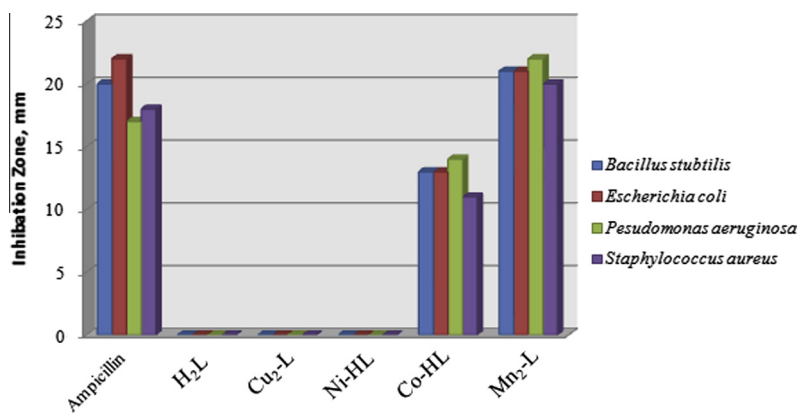
Figure 7 The antibacterial activities of Schiff base and its complexes.

Table 9 Biological activity of H_2L ligand and its metal complexes.

Tested microorganism	H_2L	Ni—HL	Co—HL	Cu_2—L	Mn_2—L	Standard Ampicillin
Gram positive bacteria						
Staphylococcus aureus	0.0	0.0	11	0.0	20	18
Bacillus subtilis	0.0	0.0	15	0.0	21	20
Gram negative bacteria						
Pseudomonas aeruginosa	0.0	0.0	14R[a]	0.0	22	17
Escherichia coli	0.0	0.0	13	0.0	21	22

[a] R = Repellent (not complete inhibition).

4. Conclusions

In this work the Schiff base ligand was prepared from condensation reaction of o-phenylenediamine and 6-formyl-7-hydro xyl-5-methoxy-2-methylbenzopyran-4-one and its complexes with metal ions Mn(II), Co(II), Ni(II) and Cu(II) are synthesized and characterized. It is concluded from analytical and spectral data that the Schiff base acts as monobasic bidentate ligand and coordinates to the central metal ions Ni(II) and Co(II) complexes via the azomethine nitrogen atom and deprotonated phenolic oxygen anion with 1:1 (M:L) stoichiometry. In 2:1 (M:L) binuclear metal chelates the Schiff base behaves as a dibasic tetradentate ligand, coordination occurring via the two azomethine nitrogen atoms and the two deprotonated phenolic oxygen anions. The mass spectra of the complexes confirm their molecular formulae. FTIR spectral and electrical conductance showed that the OH^- or Cl^- is bound to the central metal ions in the coordination sphere to complete the coordination number of the metal. The theoretical calculation shows that the four active centers are O7, O35, N9 and N17. In case of Ni—HL, Co—HL and Mn_2—L complexes, two water molecules occupy the axial positions and the other water molecule and the OH^- or Cl^- at the equatorial positions to give octahedral geometry. The binuclear Cu_2—L shows square planar geometry. All the studied complexes are polar as it is evident from the magnitude of their dipole moments. The reactivity of the metal complexes follows the order Cu_2—L > Mn_2—L > Ni—HL > Co—HL. Atomic charge calculations indicate an electric charge donated from the ligand to the metal LM as well as back-donation from the metal ion to the donating sites. Moreover, the antibacterial activities of the prepared complexes were studied. Mn_2—L complex showed the highest biological activity among the other complexes toward *S. aureus and B. Subtilis* (G^+) and *P. aeruginosa and E. coli* (G^-) bacteria.

Acknowledgments

References

Abu-Dief, A.M., Mohamed, I.M.A., 2015. A review on versatile applications of transition metal complexes incorporating Schiff bases. Beni-Suef Uni. J. Basic Appl. Sci. http://dx.doi.org/10.1016/j.bjbas.2015.05.004.

Amin, R.M., Abdel-Kader, N.S., El-Ansary, A.L., 2012. Microplate assay for screening the antibacterial activity of Schiff bases derived from substituted benzopyran-4-one. Spectrochim. Acta A 95, 517–525.

Armelao, L., Quici, S., Brigelletti, F., Accorsi, G., Bottaroi, G., Cavazzini, M., Tendello, E., 2010. Design of luminescent lanthanide complexes: from molecules to highly efficient photo-emitting materials. Coord. Chem. Rev. 254, 487–505.

Becke, A.D., 1993. Density-functional thermochemistry. iii. Rhe role of exact exchange. J. Chem. Phys. 98 (7), 5648–5652.

Bellamy, L.J., 1975. The Infrared Spectra of Complex Molecules. Champan and Hall, London.

Bolos, C.A., Nikolov, G..St., Ekateriniadou, I., Kortsaris, A., Kyriakidis, D.A., 1998. Structure-activity relationships for some diamine, triamine and Schiff base derivatives and their copper(II) complexes. Metal Based Drugs 5, 323–333.

Bradley, P.G., Kress, N., Hornberger, B.A., Dallinger, R.F., Woodruff, W.H., 1981. Vibrational spectroscopy of the electronically excited State. 5. Time-Resolved Resonance Raman Study of Tris(bipyridine)ruthenium (II) and Related Complexes. Definitive Evidence for the "Localized" MLCT State. *J. Am. Chem. Soc.* 103, 7441–7446.

Brodowska, K., odyga-Chruścińska, E., 2014. Schiff bases – interesting range of applications in various fields of science. CHEMIK 68 (2), 129–134.

Chavan, S.V., Sawant, S.S., Yamgar, R.S., 2011. Synthesis and characterization of novel transition metal complexes of Benzo-Pyranone derivatives and their biological activities. Asian J. Research Chem. 4 (5), 834–837.

Chohan, Z.H., Jaffery, M.F., 2000. Synthesis, characterization and biological evaluation of Co(II), Cu(II), Ni(II) and Zn(II) complexes with cephradine. Metal Based Drugs 7, 265–269.

Dharmaraj, N., Viswanathamurthi, P., Natarajan, K., 2001. Ruthenium(II) complexes containing bidentate Schiff bases and their antifungal activity. Trans. Met. Chem. 26, 105–109.

Di Braccio, M., Grossi, G., Roma, G., Marzano, C., Baccichetti, F., Simonato, M., Bordin, F., 2003. Pyran derivatives: part XXI. Antiproliferative and cyotoxic properties of novel N-substituted 4-aminocoumarins, their benzo-fused derivatives, and some related 2-aminochromones. Farmaco 58, 1083–1097.

Downing, R.S., Urbach, F.L., 1969. Circular dichroism of square-planar, tetradentate Schiff base chelates of copper (II). J. Am. Chem. Soc. 91 (22), 5977–5983.

Dros, A.C., Zijlstra, R.W.J., Duijnen, P.Th., Spek, A.L., Kooijman, H., Kellogg, R.M., 1998. Unusual conformational aspects of some novel chiral non-racemic pyridinyl-2-phosphonates. Tetrahedron 54, 7787–7812.

Earnshaw, A. 1968. Introduction to Magneto Chemistry, Academic press Inc.

El-Gaby, M.S.A., 2004. Syntheses of hitherto unknown thiazole, ylidene and pyridinethione derivatives having a piperidin-1-yl

moiety and their use as antimicrobial agents. J. Chin. Chem. Soc. 51, 125–134.

El-Gammal, O.A., 2010. Synthesis, characterization, molecular modeling and antimicrobial activity of 2-(2-(ethylcarbamothioyl)hydrazinyl)-2-oxo-N-phenylacetamide copper complexes. Spectrochim. Acta A 75, 533–542.

Emeleus, H.J., Sharpe, A.G., 1974. Modern Aspects of Inorganic Chemistry, fourth ed. Roultedge and Paul, London.

Frisch, M.J., Trucks, G.W. et al., 2009. Gaussian Inc., Wallingford CT.

Gaber, M., Al-Shihry, S.S., 2004. Cobalt (II), nickel (II) and copper (II) complexes of carbohydrazide and its arylidene derivatives. Sci. J. King Faisal Uni. (Basic Appl. Sci.) 5, 1425.

Gaur, S., 2003. Phsicochemical and biological properties of Mn(II), Ni(II) and chelates of Schiff bases. Asian J. Chem. 15, 250–254.

Geary, W.J., 1971. The use of conductivity measurements in organic solvents for the characterisation of coordination compounds. Coord. Chem. Rev. 7, 81–122.

Gudasi, K.B., Patil, M.S., Vadavi, R.S., Shenoy, R.V., Patil, S.A., Nethaji, M., 2006. X-Ray Crystal Structure of the N-(2-hydroxy-1-naphthalidene)phenylglycine Schiff Base. Synthesis and Characterization of Its Transition Metal Complexes. Chemistry and Materials Science. 31(5), 580–585.

Hankare, P.P., Gavali, L.V., Bhuse, V.M., Delekar, S.D., Rokade, R.S., 2004a. Synthesis and characterization of tridentate Schiff's base derived from 5-(20-thiazolylazo)salicylaldehyde and p-methoxy aniline and their Mn(II), Co(II), Ni(II), Cu(II), Zn(II), Cd(II) and Hg(II) Complexes. Indian J. Chem. 43, 2578–2581.

Hankare, P.P., Naravane, S.R., Bhuse, V.M., Delekar, S.D., Jagtap, A.H., 2004b. Synthesis and characterization of Mn(II), Co(II), Ni(II), Cu(II) and Zn (II) azo coumarin complexes. Indian J. Chem. 43A, 1464–1467.

Hay, P.J., Wadt, W.R., 1985. Ab initio efective core potentials for molecular calculations. Potentials for K to Au including the outermost core orbitals. J. Chem. Phys. 82, 299–310.

Jha, R.R., Mukharjee, P., 2007. Synthesis and characterization of transition metal complexes with 1,5-diamino-2,4-dimethyl-1,5-diaza-1,4-pentadiene. Asian J. Chem. 1, 641–646.

Junnosuke, F., Kazuo, N., Masahisa, K., 1956. Infrared spectra of metallic complexes. II. The absorption bands of coordinated water in aquo complexes. J. Am. Chem. Soc. 78 (16), 3963–3965.

Kemp, W., 1978. Inorganic spectroscopy, third ed. ELBS.

Keypour, H., Rezaeivala, M., Valencia, L., Pérez-Lourido, P., Khavasi, H.R., 2009. Synthesis and characterization of some new Co (II) and Cd (II) macroacyclic Schiff-base complexes containing piperazine moiety. Polyhedron 28 (17), 3755–3758.

Kumar, S., Koh, J., 2012. Physiochemical, optical and biological activity of chitosan-chromone derivative for biomedical applications. Int. J. Mol. Sci. 13, 6102–6116.

Kuźmin, V.E., Artemenko, A.G., Lozytska, R.N., Fedtchouk, A.S., Lozitsky, V.P., Muratov, E.N., Mescheriakov, A.K., 2005. Investigation of anticancer activity of macrocyclic Schiff bases by means of 4D-QSAR based on simplex representation of molecular structure. SAR QSAR Environ. Res. 16, 219–230.

Liu, W., Qing, C., Chen, X., Ye, Q., Yu, Y., Hou, S., 2008. Preparation, characterization and in vitro anticancer activity of platinum(II) complexes with N-Cyclohexyl-1,3-propanediamine as the carrier. Chem Pharm Bull. 56 (5), 659–662.

Macdonald, A.M.G., Sirichanya, P., 1969. The determination of metals in organic compounds by oxygen-flask combustion or wet combustion. Microchem. J. 14, 199–206.

Martens, S., Mithöfer, A., 2005. Flavones and Flavone synthases. Phytochemistry 66, 2399–2407.

McGrath, M.P., Radom, C., 1991. Extension of Gaussian-1 (G1) theory to bromine-containing molecules. J. Chem. Phys. 94, 511–516.

Nakamoto, K., 1986. Infrared and Raman Spectra of Inorganic and Coordination Compounds. Wiley, New York.

Nicholls, D., 1973. The Chemistry of Iron, Cobalt and Nickel, first ed. Pergamon Press, Oxford, England.

Patil, S.A., Unki, S.N., Badami, P.S., 2013. Synthesis, characterization, biological and thermal behavior of Co(II), Ni(II) and Cu(II) complexes with Schiff bases having coumarin moieties. J. Therm. Anal. Calorim. 111, 1281–1289.

Rakha, T.H., El-Gammal, O.A., Metwally, H.M., Abu El-Reash, G.M., 2014. Synthesis, characterization, DFT and biological studies of (Z)-N·-(2-oxoindolin-3-ylidene)picolinohydrazide and its Co(II), Ni(II) and Cu(II) complexes. J. Mol. Struct. 1062, 96–109.

Rao, C.N.R., 1963. Chemical Application of Infrared Spectroscopy. Academic Press, New York.

Saraswat, B.S., Srivastava, G., Mehrotra, R.C., 1977. Schiff base complexes of organotin (IV). Reactions of trialkyltin(IV) chlorides and alkoxides with N-substituted salicylideneimines. J. Organomet. Chem. 129 (2), 155–161.

Sherif, O.E., Abdel-Kader, N.S., 2014. Spectroscopic and biological activities studies of bivalent transition metal complexes of Schiff bases derived from condensation of1,4-phenylenediamine and benzopyrone derivatives. Spectrochim. Acta A 117, 519–526.

Sönmez, M., Sekerci, M., 2002. Synthesis and Characterization of Cu(II), Co(II), Ni(II) and Zn(II) Schiff Base Complexes from 1-Amino-5-benzoyl-4-phenyl-1H-pyrimidine-2-one with Salicylaldehyde. Polish J. Chem. 76, 907–914.

Thakor, Y.J., Patel, S.G., Patel, K.N., 2010. Synthesis, characterization and biomedical studies of some transition metal complexes containing tetra dentate and neutral bi dentate Schiff base. J. Chem. Pharm. Res. 2 (5), 518–525.

Vogel, A.I., Tatchell, A.R., Furnis, B.S., Hannaford, J.A., Smith, P.W.G., 1989. Vogel's Textbook of Practical Organic Chemistry, fifth ed. Longmans, London.

Wang, L.F., Zhu, Y., Yang, Z.Y., Wu, J.G., Wang, Q., 1991. Manganase(II) complex of a hydrazone ligand derived from pyruvic acid and 4-pyridine carboxylic acid hydrazide-synthesis and crystal structure. Polyhedron 10, 2477–2481.

Yıldırım, L.T., Kurtaran, R., Namli, H., Azaz, A.D., Atakol, O., 2007. Synthesis, crystal structure and biological activity of two new heterotrinuclear thiocyanato bridged Cu(II)–Hg(II)–Cu(II) complexes. Polyhedron 26, 4187–4194.